Int. J. Electron. Commun. (AEÜ) 86 (2018) 171–176

Contents lists available at ScienceDirect

Int. J. Electron. Commun. (AEÜ)

journal homepage: www.elsevier.com/locate/aeue

Regular paper

Non-orthogonal multiple access protocol for overlay cognitive radio networks using spatial modulation and antenna selection

Said Emam*, M.E. Çelebi

Electronics and Communications Department, Istanbul Technical University, Istanbul, Turkey

ARTICLE INFO

Keywords:
Overlay cognitive radio
Non-orthogonal multiple access
Spatial modulation
Cooperative communication
Antenna selection

ABSTRACT

In this paper we propose a novel spectrum sharing protocol for overlay cognitive radio networks using non-orthogonal multiple access (NOMA), spatial modulation (SM) and antenna selection (AS). The proposed protocol allows a secondary transmitter (ST) to transmit simultaneously to both a primary receiver (PR) and a secondary receiver (SR) using SM. The usage of NOMA and SM will increase the spectral efficiency for both PR and SR with reduced detection complexity than the case without NOMA in which the detectors are required to jointly detect both SM symbols at each receiver. The application of AS at ST with regards to PR provides higher quality transmission for PR without affecting the performance of SR. The performance of the proposed protocol is investigated by derivations of upper bounds on the average symbol error probabilities at PR and SR and by Monte Carlo simulations. Analytical and simulation results show that the proposed protocol offers efficient spectrum utilization over spectrum sharing protocols proposed recently that uses SM – to convey the primary data to PR through the amplitude phase modulation technique and the secondary data to SR through the index of the active antenna.

1. Introduction

Cognitive radio (CR) was proposed as a promising technology for enhancing the utilization of the radio spectrum, since it could efficiently resolve the spectrum scarcity versus the under-utilization dilemma caused by the conventional fixed spectrum allocation [1]. Research on CR has been divided into three main spectrum-sharing paradigms: interweave, underlay, and overlay. In this paper we consider the overlay model where the secondary users (SUs) are assumed to be equipped with advanced signal processing and encoding techniques to maintain or enhance the communication of the primary users (PUs) while also gaining access to the spectrum for their own communication [2].

To tackle the less-efficient use of the scarce spectrum various multiplexing techniques have been recently proposed, like spatial modulation (SM) and non-orthogonal multiple access (NOMA), where NOMA exploits the power domain and SM exploits the spatial domain to efficiently improve the spectrum utilization. Spatial modulation (SM) was introduced in [3] as a spatial multiplexing technique that effectively remove inter channel interference and synchronization issues amongst antennas in multiple input multiple output (MIMO) systems; since only one transmit antenna is allowed to transmit at any transmission period. SM increases the spectral efficiency by utilizing the active antenna index for conveying information besides the usage of conventional amplitude and phase modulation (APM) techniques. Inspired by SM, some variants of SM schemes have been investigated such as: spatial shift keying (SSK) that reduces the complexity of SM by utilizing the spatial domain only, and generalized spatial modulation (GSM) that increases the spectral efficiency of SM, by allowing more than one transmit antenna to be active at a time, in a tradeoff with increased receiver complexity [4,5]. For SM, the optimal maximum likelihood (ML) detector that jointly estimates the active antenna index and the transmitted APM symbol was proposed in [6]. For further improvement in the performance of SM, antenna selection (AS) was investigated. In [7], the authors proposed two AS schemes for SM systems, the Euclidean Distance optimized AS (EDAS) and Capacity Optimized AS (COAS). Both schemes were shown to provide significant performance compared with SM without AS, while EDAS outperforms COAS but with increased computational complexity [8].

The application of spatial modulation (SM) in overlay cognitive radio networks has been recently investigated. In [9], the authors considered using SM at the secondary transmitter to relay the primary transmitter APM symbol using decode-and-forward (DF) technique while the symbol intended for the secondary receiver is used to select the transmitting antenna index. The performance of the protocol is evaluated by computing upper bounds on the bit error probabilities

* Corresponding author.
E-mail addresses: emams@itu.edu.tr (S. Emam), mecelebi@itu.edu.tr (M.E. Çelebi).

https://doi.org/10.1016/j.aeue.2018.02.006
Received 9 November 2017; Accepted 2 February 2018
1434-8411/

(BEP) for single antenna primary and secondary receivers. The authors of [9] extended their work in [10] for different relaying strategies: fixed and incremental amplify and forward, and selective decode and forward, with upper bounds on the BEP have been derived. In [11], the authors considered the same idea of [9] but using amplify and forward and multiple antenna primary and secondary receivers. The performance is evaluated by deriving upper bounds for the average symbol error rates at the primary and secondary receivers.

On the other hand, NOMA with successive interference cancellation (SIC) is a promising spectrally efficient multi-user access scheme for 5G mobile networks, where multiple users are served at the same time span and frequency band, but with different power levels [12]. The performance of NOMA improves when the difference in channel gains between users is large [13]. With NOMA, users with higher channel gains are allocated less power, and hence they can decode their intended information by applying SIC. User pairing can be used to improve the performance of NOMA, by pairing the users with more distinctive channel gains with each other [14]. To further increase the spectral efficiency of NOMA, recent studies investigated the application of NOMA with multiple antenna systems, for example in [15,16] the authors studied the performance of NOMA over MIMO channels. The researchers in [17] investigated NOMA with SM in a downlink multiuser transmission and the performance has been compared with orthogonal multiple access-based SM (OMA-SM) and transmit antenna grouping based SM (TAG-SM) schemes. In [18] the authors proposed a hybrid detection scheme to combine SM and NOMA in the uplink side. The application of NOMA in CR networks has recently attracted many researchers to investigate problems related with outage probability, capacity analysis and power allocation schemes to further improve the system performance [19]. For example in [20] the authors studied the power allocation problem for NOMA-based CR networks and proposed a low complexity algorithm that guarantees the quality of service requirements for both the PUs and SUs. In [21], the researchers proposed an algorithm to maximize the energy efficiency of a generalized CR inspired NOMA system, subject to both the transmit power constraint and the QoS guarantees for all primary users.

In this paper we propose a spectrum sharing protocol for overlay CR networks using NOMA, SM and AS. The proposed protocol allows the secondary transmitter (ST) to transmit simultaneously to both the primary receiver (PR) and the secondary receiver (SR) using SM. The usage of NOMA and SM will increase the spectral efficiency for both the primary and secondary receivers. With NOMA, SR uses SIC to detect the signal intended for PR and then cancels it to detect its own signal while PR uses direct decoding to detect its own signal considering the intended signal for SR as an interference. This decreases the detection complexity considerably compared to the case without NOMA in which the detectors are required to jointly detect both SM symbols at each receiver. Furthermore, the application of AS at ST in accordance with PR will enhance the performance of PR without affecting the performance of SR. This will ensure that the primary symbol will be sent over one of the channels with high gain (with respect to PR) and the secondary symbol will be sent over one of the channels with low gain (with respect to PR), which will result in a little secondary interference at PR – compared with the case without AS – and therefore will enhance the performance of PR. On the other hand the new ordering of the antennas of ST is still random with respect to SR and hence will not affect the performance of SR on the average. The performance of the proposed protocol is investigated through derivations of upper bounds for the average symbol error probabilities (SEP) at PR and SR and through Monte Carlo simulations.

This paper is organized as follows. Section 2 presents the system model and the proposed overlay CR NOMA-SM protocol description with and without AS. The performance analysis of the primary and secondary users is presented in Section 3. The analytical and simulation results are discussed in Section 4. Finally Section 5 concludes the paper.

Notation: Throughout this paper bold lower and upper-case letters are used for vectors and matrices, respectively. $Re\{\cdot\}$ denotes the real part of a complex number. $(\cdot)^T$ and $(\cdot)^H$ are used to represent the transpose and Hermitian transpose of a vector (or a matrix), respectively. $||\boldsymbol{x}||$ is used to represent the L_2-norm of a vector $\boldsymbol{x}$. Circularly symmetric complex Gaussian random variable X with mean μ and variance σ^2 is represented by $X \sim \mathbb{C}\mathcal{N}(\mu,\sigma^2)$. $Q(\cdot)$ denotes the well-known Gaussian Q-function.

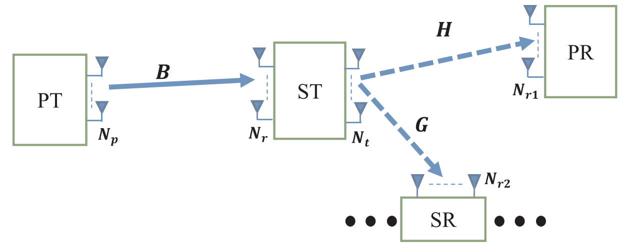

Fig. 1. System model of the overlay CR network. The solid line shows the channel matrix $\boldsymbol{B}$ and also indicates the first phase. The dashed lines show the channel matrices $\boldsymbol{H}$ and $\boldsymbol{G}$ and indicates the second phase. The black dots indicates multiple SRs that are served by ST.

2. System model

In this paper we consider an overlay cognitive radio network as shown in Fig. 1. The primary network consists of a primary transmitter (PT) with N_p transmit antennas, and a primary receiver (PR) with N_{r1} receive antennas. The secondary network consists of a secondary transmitter (ST) with N_t transmit antennas and N_r receive antennas and a secondary receiver (SR) with N_{r2} receive antennas. ST acts as a relay that cooperatively assists the communications between PT and PR while gaining access to the spectrum to convey its own information to SR. ST can be a secondary base station that needs to communicate with multiple secondary receivers, hence to achieve the most benefits of NOMA, ST is assumed to perform user pairing by selecting the SR with the highest channel gain (among all other SRs represented by dots in Fig. 1) with respect to the channel gain of the intended PR. ST uses decode and forward algorithm to relay the message of PT to PR. It is assumed that no direct link exists between PT and PR, like the case of a cell-edge user that experiences very low SNRs. Throughout this paper all nodes are constrained to operate in a half-duplex mode. We assume independent Rayleigh fading for all transmitter–receiver pairs. The channel matrices for the PT-ST, ST-PR, and ST-SR links are $\boldsymbol{B}$, $\boldsymbol{H}$ and $\boldsymbol{G}$ with entries $b_{ij} \sim \mathbb{C}\mathcal{N}(0,1)$, $h_{ij} \sim \mathbb{C}\mathcal{N}(0,\sigma_h^2)$ and $g_{ij} \sim \mathbb{C}\mathcal{N}(0,\sigma_g^2)$ respectively. Furthermore, the noise at any node is modeled as $\mathbb{C}\mathcal{N}(0,\sigma_n^2)$. P_p and P_s are the transmit powers of PT and ST, respectively. It is assumed that perfect channel state information (CSI) is available at all receivers.

As shown in Fig. 1, the communication process can be done in two phases as follows:

2.1. The first phase

PT is considered to use SM to transmit its message to ST. With SM PT divides its message into two parts, the first part ($\log_2 M$) bits select a symbol x_q from the M-ary constellation set, while the second part ($\log_2 N_p$) bits select antenna i out of N_p transmit antennas to transmit the selected symbol x_q. Hence the received signal at the receiving antennas of ST can be written as:

$$\boldsymbol{y}_{ST} = \sqrt{P_p}\boldsymbol{b}_i x_q + \boldsymbol{n}_{ST} \quad (1)$$

where $\boldsymbol{b}_i (1 \leqslant i \leqslant N_p)$ is the i^{th} column of $\boldsymbol{B}$ and represents the channel vector between the active antenna at PT and the receiving antennas at ST. $\boldsymbol{n}_{ST}$ is the noise vector at ST. For equally likely symbols, the optimal detector at ST based on the ML principle is given as:

$$[\hat{i},\hat{q}] = \underset{i',q'}{\operatorname{argmin}} \|\boldsymbol{y}_{ST} - \sqrt{P_p}\boldsymbol{b}_{i'}x_{q'}\|^2 \tag{2}$$

where $1 \leqslant i' \leqslant N_p$, and $1 \leqslant q' \leqslant M$.

2.2. The second phase

In this phase, if ST successfully decodes the message of PT in the first phase, it generates two messages using NOMA and SM which are transmitted to both PR and SR simultaneously. ST splits its N_t transmitting antennas into two groups, N_{t1} antennas for SM for PR, while the remaining antennas ($N_{t2} = N_t - N_{t1}$) are used for SM for SR. Then ST uses NOMA-SM to transmit simultaneously to both users. Using NOMA, ST splits its transmit power P_s between the two users according their channel gain strengths. After correct power allocation, ST transmits simultaneously the detected primary message from first phase with power portion P_{s1} for PR (encoded using SM with the N_{t1} antennas group and the suitable APM symbol), and a new message with power portion P_{s2} for SR (encoded using SM with the N_{t2} antennas group), where $P_{s1} + P_{s2} = P_s$. We refer to this mode of transmission as *CR NOMA-SM without AS*. The splitting of the transmitting antennas depends on the required rates at both PR and SR. For example, if the required rates at both PR and SR are 4 and 3 bpcu (bits per channel use), respectively, and $N_t = 6$. One possible scenario at ST is to assign $N_{t1} = 4$ with QPSK to provide 2 bit of information through the active antenna index and 2 bits of information through the APM technique. The remaining 2 antennas and using QPSK can be assigned to SR to provide the required 3 bits of information.

To enhance the quality of service for PR we propose the use of COAS [7], where PR computes the indices corresponding to the N_{t1} largest channel norms out of the N_t antennas of ST for every coherence interval and feeds it back to ST. Then it is the responsibility of ST to transmit the new ordering information of the antennas to SR, where this can be done during the first phase through the use of feedback control channels. The ordering can be given as follows:

$$\underbrace{\|\boldsymbol{h}_{(1)}\|^2 \geqslant \|\boldsymbol{h}_{(2)}\|^2 \geqslant \ldots \geqslant \|\boldsymbol{h}_{(N_{t1})}\|^2}_{\text{Largest } N_{t1} \text{channel norms}} \geq \underbrace{\|\boldsymbol{h}_{(N_{t1}+1)}\|^2,\ldots,\|\boldsymbol{h}_{(N_t)}\|^2}_{\text{Ordering is arbitrary}}$$

where $\boldsymbol{h}_{(j)}$ indicates the j^{th} column of $\boldsymbol{H}$ with the new ordering. With this AS the N_{t1} antennas with the largest channel gains with respect to PR will be used for SM toward PR and the remaining N_{t2} antennas will be used for SM toward SR. Therefore using the antennas with high channel gains (with respect to PR) for SM toward PR and the antennas with low channel gains (from the perspective of PR) for SM toward SR will result in reducing the secondary symbol interference at PR, thus enhancing its performance. At SR this antenna re-indexing is random with respect to the channel matrix $\boldsymbol{G}$, which will result in no change in the performance of SR on the average. After performing AS the proposed protocol uses NOMA-SM as described in the CR NOMA-SM without AS mode. Hence we refer to this mode of transmission as *CR NOMA-SM with AS*. Therefore, the received signal at PR can be expressed as:

$$\boldsymbol{y}_{PR} = \sqrt{P_{s1}}\boldsymbol{h}_{(j)}x_p + \sqrt{P_{s2}}\boldsymbol{h}_{(k)}x_s + \boldsymbol{n}_{PR} \tag{3}$$

where $(j)(1 \leqslant (j) \leqslant N_{t1})$ and $(k)(N_{t1}+1 \leqslant (k) \leqslant N_t)$ represent the indices of the activated antennas at ST. $\boldsymbol{h}_{(j)}$ and $\boldsymbol{h}_{(k)}$ are the j^{th} and k^{th} columns of $\boldsymbol{H}$ with the new ordering, respectively, representing the channel vectors between the activated antennas (at ST) and PR. x_p and x_s are the p^{th} $(1 \leqslant p \leqslant M_1)$ and s^{th} $(1 \leqslant s \leqslant M_2)$ APM symbols intended for PR and SR, respectively. M_1-ary and M_2-ary constellations are used for PR and SR, respectively. PR decodes its intended message directly considering the message intended for SR as an interference. For equally likely symbols, the optimal detector at PR is based on the ML principle:

$$[\widehat{(j)},\hat{p}] = \underset{(j)',p'}{\operatorname{argmin}} \|\boldsymbol{y}_{PR} - \sqrt{P_{s1}}\boldsymbol{h}_{(j)'}x_{p'}\|^2 \tag{4}$$

where $1 \leqslant (j)' \leqslant N_{t1}$, and $1 \leqslant p' \leqslant M_1$.

The received signal at SR is expressed as:

$$\boldsymbol{y}_{SR} = \sqrt{P_{s1}}\boldsymbol{g}_{(j)}x_p + \sqrt{P_{s2}}\boldsymbol{g}_{(k)}x_s + \boldsymbol{n}_{SR} \tag{5}$$

where $\boldsymbol{g}_{(j)}$ and $\boldsymbol{g}_{(k)}$ are the j^{th} and k^{th} columns of $\boldsymbol{G}$ with the new ordering, respectively, representing the channel vectors between the activated antennas and SR. $\boldsymbol{n}_{SR}$ is the noise vector at SR. SR will use SIC to decode the SM symbol intended for PR and then cancels it from the received signal $\boldsymbol{y}_{SR}$ to obtain:

$$\boldsymbol{y}'_{SR} = \boldsymbol{y}_{SR} - \sqrt{P_{s1}}\boldsymbol{g}_{\widehat{(j)}}x_{\hat{p}} \tag{6}$$

where $\widehat{(j)}$ and $\hat{p}$ are the estimated antenna index and the estimated APM symbol intended for PR at SR. From $\boldsymbol{y}'_{SR}$ SR decodes its own SM symbol using ML detector as:

$$[\widehat{(k)},\hat{s}] = \underset{(k)',s'}{\operatorname{argmin}} \|\boldsymbol{y}'_{SR} - \sqrt{P_{s2}}\boldsymbol{g}_{(k)'}x_{s'}\|^2 \tag{7}$$

3. Performance analysis

In this section, the performance of the proposed protocol is investigated by deriving an upper bound for the average symbol error probability (SEP) of each link for the CR NOMA-SM without AS protocol, which also can be considered as an upper bound for the CR NOMA-SM with AS protocol.

3.1. The SEP of the PT − ST link

Since the PT − ST link is using SM, the upper bound for the average SEP can be derived from (2) as in [6] using the well-known union bounding technique as follows:

$$\overline{SEP}_{PT\to ST} \leqslant \frac{1}{MN_p}\sum_{\substack{i=1\\ iq \neq i'q'}}^{N_p}\sum_{q=1}^{M}\sum_{i'=1}^{N_p}\sum_{q'=1}^{M}\omega^{N_r} \times \sum_{l=0}^{N_r-1}\binom{N_r-1+l}{l}(1-\omega)^l \tag{8}$$

where $\omega = \frac{1}{2}\left(1-\sqrt{\frac{\sigma_q^2}{1+\sigma_q^2}}\right)$, and $\sigma_q^2 = \frac{P_p(|x_q|^2+|x_{q'}|^2)}{4\sigma_n^2}$.

3.2. The SEP of the ST − PR link

An upper bound for the average SEP of the ST − PR link can be derived using the union bounding technique as follows:

$$\overline{SEP}_{ST\to PR} \leqslant \frac{1}{M_1N_{t1}}\sum_{\substack{j=1\\ jp\neq j'p'}}^{N_{t1}}\sum_{p=1}^{M_1}\sum_{j'=1}^{N_{t1}}\sum_{p'=1}^{M_1}\overline{PEP}_{ST\to PR} \tag{9}$$

where $(1 \leqslant j,j' \leqslant N_{t1})$, $(1 \leqslant p,p' \leqslant M_1)$, and $\overline{PEP}_{ST\to PR}$ is the average pairwise error probability (PEP) at PR of deciding that the symbol $x_{p'}$ is transmitted from the j'^{th} transmit antenna given that the symbol x_p was transmitted from the j^{th} transmit antenna of ST.

The instantaneous PEP at PR ($PEP^i_{ST\to PR}$) conditioned on H can be computed by rewriting (3) as follows:

$$\boldsymbol{y}_{PR} = \sqrt{P_{s1}}\boldsymbol{h}_jx_p + \tilde{\boldsymbol{n}}\,(10) \tag{10}$$

where $\tilde{\boldsymbol{n}} = \sqrt{P_{s2}}\boldsymbol{h}_kx_s + \boldsymbol{n}_{PR}$. Conditioned on knowing $\boldsymbol{H}$ at PR, $\tilde{\boldsymbol{n}}$ is the interference plus noise vector with each component is a complex Gaussian random variable with variance $(P_{s2}\sigma_h^2 + \sigma_n^2)$. By using (4), $PEP^i_{ST\to PR}$ can be written as:

$$PEP^i_{ST\to PR} = P(d_{jp} > d_{j'p'}|\boldsymbol{H}) = P(\widetilde{N} > P_{s1}\|\boldsymbol{h}_j x_p - \boldsymbol{h}_{j'}x_{p'}\|^2|\boldsymbol{H})$$
$$= Q\left(\sqrt{\frac{P_{s1}\|\boldsymbol{h}_j x_p - \boldsymbol{h}_{j'}x_{p'}\|^2}{2(P_{s2}\sigma_h^2+\sigma_n^2)}}\right) = Q(\sqrt{\gamma}) \quad (11)$$

where $d_{jp} = \|y_{PR} - \sqrt{P_{s1}}\boldsymbol{h}_j x_p\|^2$, $\widetilde{N} = 2Re\{\widetilde{\boldsymbol{n}}^H\sqrt{P_{s1}}(\boldsymbol{h}_j x_p - \boldsymbol{h}_{j'}x_{p'})\}$ is a real Gaussian random variable with zero mean and variance $(2(P_{s2}\sigma_h^2+\sigma_n^2)P_{s1}\|\boldsymbol{h}_j x_p - \boldsymbol{h}_{j'}x_{p'}\|^2)$, and

$$\gamma = \frac{P_{s1}\|\boldsymbol{h}_j x_p - \boldsymbol{h}_{j'}x_{p'}\|^2}{2(P_{s2}\sigma_h^2+\sigma_n^2)} = \frac{P_{s1}\sum_{i=1}^{N_r}\|h_{ij}x_p - h_{ij'}x_{p'}\|^2}{2(P_{s2}\sigma_h^2+\sigma_n^2)} \quad (12)$$

To obtain the average pairwise error probability ($\overline{PEP}_{ST\to PR}$) we take the average of ($PEP^i_{ST\to PR}$) over the PDF of the random variable γ. The PDF of the random variable γ is difficult to be obtained for the general case when x_p is drawn from complex constellation since the real and imaginary parts of the complex random variable $(h_{ij}x_p - h_{ij'}x_{p'})$ in (12) are not independent. Following the procedure in [6], for independence to be satisfied we consider the case when x_p is drawn from real constellation. Hence (12) reduces to $\gamma = \sum_{l=1}^{2N_{r1}} v_l^2$, where v_l is a zero mean Gaussian random variable with variance $\sigma_v^2 = \frac{P_{s1}\sigma_h^2(\|x_p\|^2+\|x_{p'}\|^2)}{4(P_{s2}\sigma_h^2+\sigma_n^2)}$. Therefore the random variable γ is a chi-square random variable with $2N_{r1}$ degrees of freedom. Then the average PEP can be obtained as in [6,22]

$$\overline{PEP}_{ST\to PR} = \int_0^\infty PEP^i_{ST\to PR}P_\gamma(\gamma)d\gamma = \mu^{N_{r1}}\sum_{l=0}^{N_{r1}-1}\binom{N_{r1}-1+l}{l}(1-\mu)^l \quad (13)$$

where $\mu = \frac{1}{2}\left(1-\sqrt{\frac{\sigma_v^2}{1+\sigma_v^2}}\right)$. By plugging (13) in (9) we obtain the upper bound for the average SEP of the ST-PR link.

3.3. The SEP of the ST − SR link

As we mentioned in Section 2 that SR uses SIC to decode first the primary message and then cancels it to decode its own intended message. Therefore the average SEP of the ST − SR link can be upper bounded by the summation of the average SEP of decoding the primary SM symbol at SR ($\overline{SEP}^{(p)}_{ST\to SR}$) and the average SEP of decoding the secondary SM symbol conditioned on correct decoding of the primary SM symbol at SR ($\overline{SEP}^{(s)}_{ST\to SR}$) as follows:

$$\overline{SEP}_{ST\to SR} \leqslant \Pr([\hat{j},\hat{p}] \neq [j,p]) + \Pr([\hat{k},\hat{s}] \neq [k,s]|[\hat{j},\hat{p}] = [j,p])$$
$$= \overline{SEP}^{(p)}_{ST\to SR} + \overline{SEP}^{(s)}_{ST\to SR} \quad (14)$$

Following similar procedure that is used at PR we can derive the average PEP in each stage in the SIC at SR ($\overline{PEP}^{(p)}_{ST\to SR}, \overline{PEP}^{(s)}_{ST\to SR}$) and hence the upper bounds for the average SEP in each stage ($\overline{SEP}^{(p)}_{ST\to SR}, \overline{SEP}^{(s)}_{ST\to SR}$), as follows:

$$\overline{PEP}^{(p)}_{ST\to SR} = \alpha^{N_{r1}}\sum_{l=0}^{N_{r1}-1}\binom{N_{r1}-1+l}{l}(1-\alpha)^l \quad (15)$$

where $\alpha = \frac{1}{2}(1-\sqrt{\frac{\sigma_w^2}{1+\sigma_w^2}}), \sigma_w^2 = \frac{P_{s1}\sigma_g^2(|x_p|^2+|x_{p'}|^2)}{4(P_{s2}\sigma_g^2+\sigma_n^2)}$. Then

$$\overline{SEP}^{(p)}_{ST\to SR} \leqslant \frac{1}{M_1 N_{t1}}\sum_{\substack{j=1\\ jp\neq j'p'}}^{N_{t1}}\sum_{p=1}^{M_1}\sum_{j'=1}^{N_{t1}}\sum_{p'=1}^{M_1}\overline{PEP}^{(p)}_{ST\to SR} \quad (16)$$

And

$$\overline{PEP}^{(s)}_{ST\to SR} = \beta^{N_{r2}}\sum_{l=0}^{N_{r2}-1}\binom{N_{r2}-1+l}{l}(1-\beta)^l \quad (17)$$

where $\beta = \frac{1}{2}\left(1-\sqrt{\frac{\sigma_z^2}{1+\sigma_z^2}}\right), \sigma_z^2 = \frac{P_{s2}\sigma_g^2(\|x_s\|^2+\|x_{s'}\|^2)}{4\sigma_n^2}$. Then

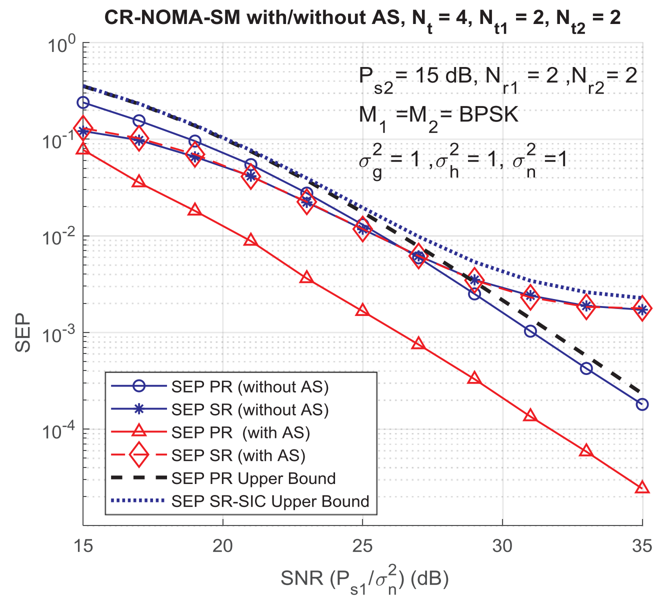

Fig. 2. The performance of the proposed protocol at PR and SR with equal channel variances.

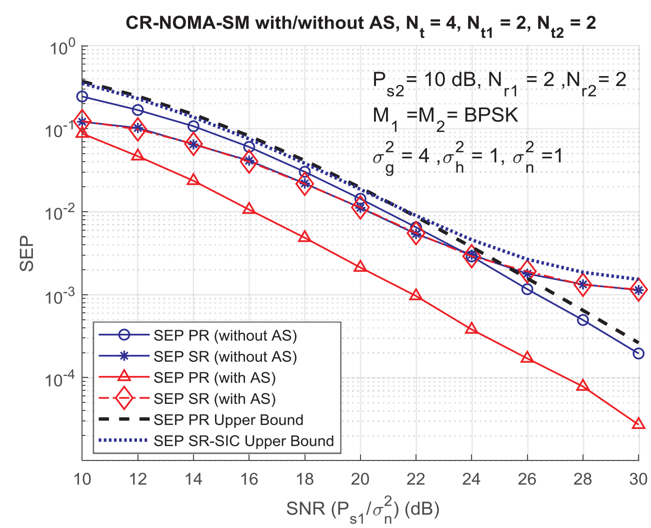

Fig. 3. The performance of the proposed protocol at PR and SR with distinctive channel variances.

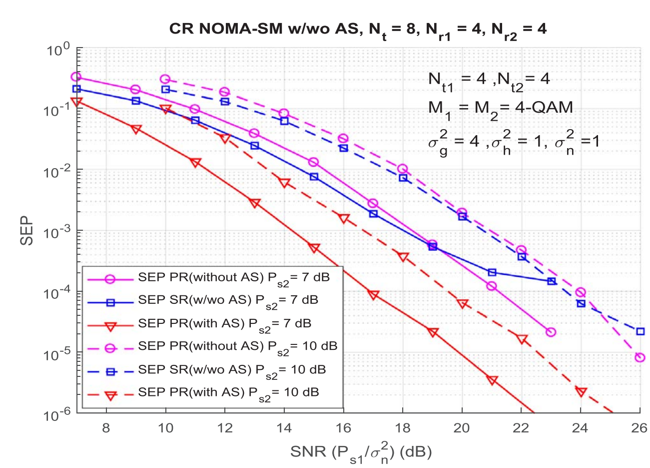

Fig. 4. The performance of the proposed protocol at PR and SR with increased transmit antennas at ST and increased receiving antennas at PR and SR. using QPSK and different transmit powers for the secondary SM symbol.

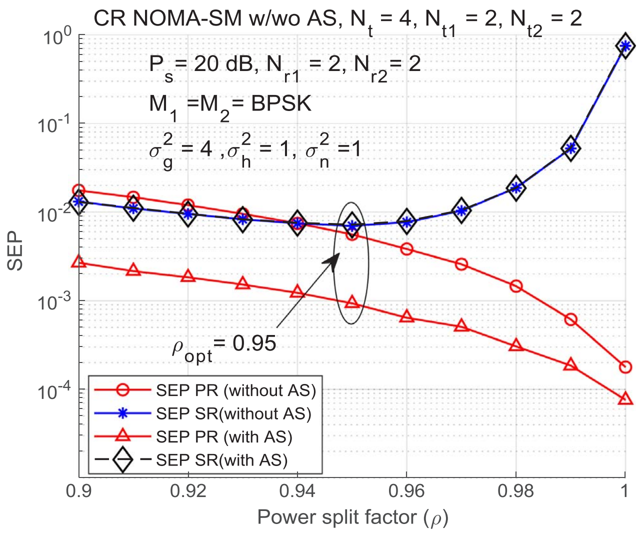

Fig. 5. The SEP for PR and SR vs the power split factor ρ for $P_s = 20\,dB$.

$$\overline{SEP}^{(s)}_{ST\to SR} \leqslant \frac{1}{M_2 N_{t2}} \sum_{\substack{k = N_{t1}+1 \\ ks \neq k's'}}^{N_t} \sum_{s=1}^{M_2} \sum_{k'=N_{t1}+1}^{N_t} \sum_{s'=1}^{M_2} \overline{PEP}^{(s)}_{ST\to SR} \tag{18}$$

By plugging (16) and (18) into (14) we obtain the overall upper bound for the average SEP of the ST − SR link.

4. Results and discussion

In this section we evaluate the performance of the proposed protocol at the primary and secondary receivers via analytical and Monte Carlo simulations for the CR NOMA-SM protocol with and without AS for different values of system parameters.

Fig. 2 shows the analytical and simulation SEP performance at both PR and SR for target rates 2 bpcu for each user for the CR NOMA-SM protocol with/without AS for system parameters: $N_t = 4, N_{t1} = N_{t2} = 2, N_{r1} = N_{r2} = 2$, using BPSK for both users, with equal channel variances $\sigma_g^2 = \sigma_h^2 = 1$, and $P_{s2} = 15$ dB. We can see that the analytical results agree with the simulation results. Also, we can see that, to achieve average SEP of 10^{-3} at PR, by using AS, the performance of PR is improved by around 5 dB compared to the case of without AS. On the other hand we observe that the performance of SR does not change in both cases as expected. Also the SEP of SR appears to be constant at high SNRs of the primary symbol, since P_{s2} is fixed and SIC is almost perfect.

In Fig. 3, we study the performance of the protocol at PR and SR for distinctive channel strengths. We repeat the simulation with the same parameters as in Fig. 2, except $\sigma_g^2 = 4$ and $P_{s2} = 10$ dB. Since the channel for SR is better than PR, ST assigns less power for the SR symbol than that for it in the previous case of equal channel gains. Fig. 3 shows that at $P_{s1} = 26$ dB and $P_{s2} = 10$ dB the SEP of PR without AS is approximately 10^{-3} and with AS it is approximately 2×10^{-4}, and the SEP for SR with/without AS is approximately 2×10^{-3}, while these values were obtained in Fig. 2, at $P_{s1} = 31$ dB and $P_{s2} = 15$ dB, i.e. by pairing the users with distinctive channel strengths such that $\sigma_g^2 = 4$, and $\sigma_h^2 = 1$ provide around 5 dB gain in the power assigned for both PR and SR symbols.

Fig. 4 shows the performance of the protocol with increased transmit antennas at ST, increased receiving antennas at PR and SR and using QPSK. The system parameters are: $N_t = 8$, $N_{t1} = N_{t2} = 4$, $N_{r1} = N_{r2} = 4$, $\sigma_g^2 = 4, \sigma_h^2 = 1$ and at different values of P_{s2} (7 dB and 10 dB). The target rates are 4 bpcu for both users. We can observe that the protocol performs well with increased numbers of transmit and receive antennas and using QPSK. We can observe that for PR the results with $P_{s2} = 7$ dB is better than the case with $P_{s2} = 10$ dB since less power for the SR symbol results in less interference at PR and hence the performance will be improved in both cases with and without AS. On the other hand, for SR we can observe that at low SNRs of the primary symbol the results with $P_{s2} = 7$ dB is better than that with $P_{s2} = 10$ dB since for SIC at SR the interference of the SR symbol is influential and therefore low values of P_{s2} is preferred. While at higher SNRs of the primary symbol the performance of SR at $P_{s2} = 10$ dB is better than at $P_{s2} = 7$ dB since for SIC at SR the interference of the SR symbol is somehow negligible and thus SR can decode the primary SM symbol with very low error probability and then decode its own symbol with better error performance at higher values of P_{s2}.

To study the performance of power allocation, Fig. 5 shows the SEP for both PR and SR vs the power split factor ρ, where $P_{s1} = \rho P_s$,

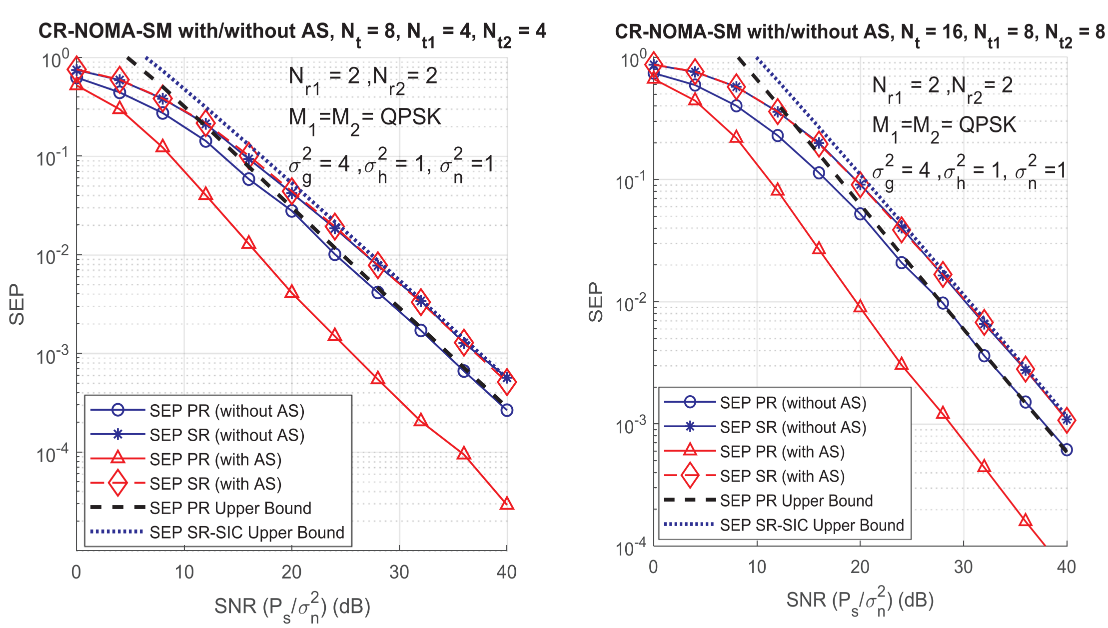

(a) 4 bpcu rates for both users (b) 5 bpcu rates for both users

Fig. 6. The SEP for PR and SR vs P_s.

$P_{s2} = (1-\rho)P_s$ and $0 \leqslant \rho \leqslant 1$, for $P_s = 20$ dB, $N_t = 4$, $N_{t1} = N_{t2} = 2$, $N_{r1} = N_{r2} = 2$, $\sigma_g^2 = 4$ and $\sigma_h^2 = 1$ and using BPSK for both users. We can see that for $P_s = 20$ dB the best value for ρ is 0.95. With this value of ρ we have the SEP of SR is the same with and without AS, and the SEP performance of PR enhanced from 5.5×10^{-3} (without AS) to 9×10^{-4} (with AS). As the transmit power P_s of ST increases to 25 dB, we find that the optimum value of ρ also increases to 0.97, the SEP of SR is the same with and without AS, and the SEP performance of PR enhanced from 2×10^{-3} (without AS) to 3×10^{-4} (with AS). We can observe that most of the transmit power is assigned to the primary symbol while less power is assigned to the secondary symbol since the channel of SR is better than that of PR. Also as P_s increases ρ_{opt} increases and at the same time P_{s2} increases which results in enhanced SEP performance for PR and SR.

Fig. 6 shows the SEP of PR and SR vs P_s, considering fairness between PR and SR by assuming the same receiving SNR of PR and SR after SIC, i.e., $\frac{P_{s1}\sigma_h^2}{P_{s2}\sigma_h^2 + \sigma_n^2} = \frac{P_{s2}\sigma_g^2}{\sigma_n^2}$. By setting $P_{s1} = \rho P_s$, and $P_{s2} = (1-\rho)P_s$, where $0 \leqslant \rho \leqslant 1$, we can obtain ρ as a function of P_s as: $\rho = \frac{B - \sqrt{(B)^2 - 4AC}}{2A}$, where $A = P_s\sigma_g^2\sigma_h^2$, $B = 2A + (\sigma_g^2 + \sigma_h^2)\sigma_n^2$, and $C = (P_s\sigma_h^2 + \sigma_n^2)\sigma_g^2$. Fig. 6(a) and (b) shows the performance of the proposed protocol for rates 4 and 5 bpcu for both PR and SR, respectively, at $N_t = 8$ and 16, $N_{t1} = N_{t2} = \frac{N_t}{2}$, $N_{r1} = N_{r2} = 2$, $\sigma_g^2 = 4$ and $\sigma_h^2 = 1$ and using QPSK for both users. We first observe that the upper bounds apply for QPSK and provides tight bounds. We also observe that with this power allocation scheme the performance enhances for both PR and SR as P_s increases. Also, the application of AS results in improving the performance of PR by around 9 dB gain in P_s at SEP of 10^{-3} in both figures without affecting the performance of SR which makes our proposed protocol provides improvements compared to protocols recently proposed.

5. Conclusions

In this paper, a novel spectrum sharing protocol that uses NOMA, SM and AS for the overlay cognitive radio network is proposed. The proposed protocol allows a secondary transmitter to transmit simultaneously to both a primary and a secondary receivers using SM, utilizing both the modulation technique and the indices of the active antennas of the secondary transmitter. The use of NOMA and SM increases the spectral efficiency of the network, and the application of AS improves the performance of the primary receiver without affecting the performance of the secondary receiver. Upper bounds on the average symbol error probabilities at the primary and secondary receivers have been derived. Analytical and simulation results show that the proposed protocol offers efficient spectrum utilization and therefore higher system capacity over the spectrum sharing protocols that use SM to convey the primary data through modulation to the primary receiver and the secondary data to the secondary receiver through the indices of the active antennas. Also the proposed protocol offers higher performance than NOMA-SM protocol without AS by utilizing AS at the secondary transmitter in accordance with the primary receiver.

References

[1] Haykin S. Cognitive radio: brain-empowered wireless communications. IEEE J Select Areas Commun 2005;23(2):201–20.

[2] Goldsmith A, Jafar SA, Maric I, Srinivasa S. Breaking spectrum gridlock with cognitive radios: an information theoretic perspective. Proc IEEE 2009;97(5):894–914.

[3] Mesleh R, Haas H, Sinanovic S, Ahn C, Yun S. Spatial modulation. IEEE Trans Veh Technol 2008;57(4):2228–42.

[4] Öztoprak ÖC, Yarkin F, Altunbas I, Basar E. Performance analysis of space shift keying for AF relaying with relay selection. AEU – Int J Electron Commun 2017;81:74–82.

[5] Castillo-Soria FR et al. Multiuser MIMO downlink transmission using block diagonalization and generalized spatial modulation techniques. AEU – Int J Electron Commun 2016;70:1228–34.

[6] Jeganathan J, Ghrayeb A, Szczecinski L. Spatial modulation: optimal detection and performance analysis. IEEE Commun Lett 2008;12(8):545–7.

[7] Rajashekar R, Hari KVS, Hanzo L. Antenna selection in spatial modulation systems. IEEE Commun Lett 2013;17(3):521–4.

[8] Pillay N, Xu H. Comments on "Antenna selection in spatial modulation systems". IEEE Commun Lett 2013;17(9):1681–3.

[9] Üstünbaş S, Başar E, Aygölü Ü. Performance analysis of cooperative spectrum sharing for cognitive radio networks using spatial modulation at secondary users. In: 2016 IEEE 83rd vehicular technology conference (VTC Spring), Nanjing; 2016. p. 1–5.

[10] Üstünbaş S, Başar E, Aygölü Ü. A cooperative spectrum sharing protocol using spatial modulation. IET Commun; April 2017.

[11] Alizadeh A, Bahrami HR, Maleki M. Performance analysis of spatial modulation in overlay cognitive radio communications. IEEE Trans Commun 2016;64(8).

[12] Li, Lan Y, Chen X, Jiang H. Non-orthogonal multiple access (NOMA) for future downlink radio access of 5G, in China. Communications 2015;12(Suppl):28–37.

[13] Benjebbour, Saito Y, Kishiyama Y, Li A, Harada A, Nakamura T. Concept and practical considerations of non-orthogonal multiple access (NOMA) for future radio access. In: 2013 International symposium on intelligent signal processing and communication systems, Naha; 2013. p. 770–4.

[14] Al-Abbasi ZQ, So DKC. User-pairing based non-orthogonal multiple access (NOMA) system. In: 2016 IEEE 83rd vehicular technology conference (VTC Spring), Nanjing; 2016. p. 1–5.

[15] Zeng M, Yadav A, Dobre OA, Tsiropoulos GI, Poor HV. On the sum rate of MIMO-NOMA and MIMO-OMA systems. IEEE Wireless Commun Lett 2017;6(4):534–7.

[16] Chinnadurai S, et al. User clustering and robust beamforming design in multicell MIMO-NOMA system for 5G communications. AEU – Int J Electron Commun 2017;78:181–91.

[17] Zhu X, Wang Z, Cao J. NOMA-based spatial modulation. In: IEEE access, vol. 5; 2017. p. 3790–800.

[18] Siregar RF, Murti FW, Shin SY. Combination of spatial modulation and non-orthogonal multiple access using hybrid detection scheme. In: 2017 Ninth international conference on ubiquitous and future networks (ICUFN), Milan; 2017. p. 476–81.

[19] Cai Y, Qin Z, Cui F, Li GY, McCann JA. Modulation and multiple access for 5G networks. In: IEEE communications surveys & tutorials, vol. PP, no. 99. http://dx.doi.org/10.1109/COMST.2017.2766698.

[20] Zeng M, Tsiropoulos GI, Dobre OA, Ahmed MH. Power allocation for cognitive radio networks employing non-orthogonal multiple access. In: 2016 IEEE global communications conference (GLOBECOM), Washington, DC; 2016. p. 1–5.

[21] Zhang Y, Yang Q, Zheng TX, Wang HM, Ju Y, Meng Y. Energy efficiency optimization in cognitive radio inspired non-orthogonal multiple access. In: 2016 IEEE 27th annual international symposium on personal, indoor, and mobile radio communications (PIMRC), Valencia; 2016. p. 1–6.

[22] Simon MK, Alouini MS. Digital communication over fading channels. 2nd ed. Piscataway, NJ, USA: Wiley/IEEE Press; 2005.